NASA/TM—1998-208664

High Strain Rate Deformation Modeling of a Polymer Matrix Composite

Part II—Composite Micromechanical Model

Robert K. Goldberg
Lewis Research Center, Cleveland, Ohio

Donald C. Stouffer
University of Cincinnati, Cincinnati, Ohio

National Aeronautics and
Space Administration

Lewis Research Center

October 1998

Acknowledgments

The authors would like to acknowledge Fiberite, Inc. for providing the material used for the experimental tests on the IM7/977-2 system along with additional information and data. The authors would also like to acknowledge Cincinnati Testing Laboratories, Inc. for conducting the tensile tests on the IM7/977-2 material presented in this report.

Available from

NASA Center for Aerospace Information
7121 Standard Drive
Hanover, MD 21076
Price Code: A03

National Technical Information Service
5285 Port Royal Road
Springfield, VA 22100
Price Code: A03

High Strain Rate Deformation Modeling of a Polymer Matrix Composite: Part II-Composite Micromechanical Model

Robert K. Goldberg
National Aeronautics and Space Administration
Lewis Research Center
Cleveland, Ohio 44135

and

Donald C. Stouffer
University of Cincinnati
Cincinnati, Ohio 45221

SUMMARY

Recently applications have exposed polymer matrix composite materials to very high strain rate loading conditions, requiring an ability to understand and predict the material behavior under these extreme conditions. In this second paper of a two part report, a three-dimensional composite micromechanical model is described which allows for the analysis of the rate dependent, nonlinear deformation response of a polymer matrix composite. Strain rate dependent inelastic constitutive equations utilized to model the deformation response of a polymer are implemented within the micromechanics method. The deformation response of two representative laminated carbon fiber reinforced composite materials with varying fiber orientation has been predicted using the described technique. The predicted results compare favorably to both experimental values and the response predicted by the Generalized Method of Cells, a well-established micromechanics analysis method.

LIST OF SYMBOLS

D_o	inelastic material constant representing maximum inelastic strain rate
E	elastic modulus of material
G	shear modulus of material
kf	fiber volume ratio of composite
n	inelastic material constant representing rate dependence of material
q	inelastic material constant representing hardening rate of material
S_{ij}	compliance matrix components
s_{ij}	deviatoric stress components
Z_o	material constant representing initial isotropic hardness of material
ε_{ij}	strain tensor components
ε^I_{ij}	inelastic strain components
ε_e^I	effective inelastic strain

ν Poisson's ratio
γ_{ij} engineering shear strain components
Ω_{ij} back stress component
Ω_m inelastic material constant representing value of back stress at saturation
σ_{ij} stress tensor components
• quantities with dots above them represent rates

Subscripts

Af bottom left subcell of composite unit cell (fiber material)
Am bottom right subcell of composite unit cell (matrix material)
B1 top left subcell of composite unit cell (matrix material)
B2 top right subcell of composite unit cell (matrix material)
A region of composite unit cell consisting of subcells Af and Am
B region of composite unit cell consisting of subcells B1 and B2
A′ region of composite unit cell consisting of subcells Af and B1
B′ region of composite unit cell consisting of subcells Am and B2
f fiber related material property
m matrix related material property
11,22,33 normal stress or strain components
12,13,23 shear stress or strain components

INTRODUCTION

NASA Lewis Research Center has an ongoing research program to develop new technologies to improve aircraft engine fan containment systems. The program contains a feasibility study to replace metallic containment systems with hardwall containment systems composed of polymer matrix composites. In such an application, the composite would be loaded at strain rates up to several hundred per second. In designing a containment system composed of polymer matrix composites, the ability to correctly model the constitutive and failure behavior of the composite under the high rate loading condition is of critical importance.

Experimental techniques to characterize the behavior of polymer matrix composites under low strain rate loading conditions have been well established for many years. Furthermore, numerous analytical techniques have been developed to model the constitutive and failure behavior of composites under quasi-static loads. However, the analytical methods required to characterize and model the constitutive and failure behavior of polymer matrix composites under high strain rates are not nearly as well developed as for quasi-static loads. Furthermore, the effects of strain rate on the material properties and response is still an area of active investigation. In addition, composites composed of more ductile matrix materials are likely to be used in high strain rate impact applications. The deformation response of these materials is likely to be nonlinear. The

majority of the modeling efforts for polymer matrix composites, however, have assumed linear elastic material response.

This paper, the second of a two-part report, describes the development of a composite micromechanical model, which allows for the analysis of the rate dependent, nonlinear deformation response of a polymer matrix composite. In composite micromechanical modeling, the effective properties and response of a composite are computed based on the properties and response of the individual constituents. To analyze the behavior of the polymer matrix constituent, strain rate dependent inelastic constitutive equations were utilized. These equations and their application are described in a companion paper [1].

This report begins with some background information. A summary of the detailed literature review given in [1], which describes previous efforts to model the rate dependent response of polymer matrix composites, will be discussed. Furthermore, an overview of the micromechanical analysis techniques that have been developed by previous researchers will be given.

After the background section, a brief overview of the constitutive equations utilized to model the deformation response of the polymer matrix will be discussed. Next, the micromechanics techniques utilized to predict the effective properties and response of the composite will be described in detail. These equations are designed to predict the response of a composite ply at an arbitrary fiber orientation angle. The numerical implementation of the methodology will also be discussed.

Finally, results predicted using the described micromechanics technique will be presented and discussed. The deformation response of two representative carbon fiber reinforced polymer matrix composites, Fiberite IM7/977-2 and AS4/PEEK, will be included. Tensile stress-strain curves for both materials will be computed for a variety of fiber orientations and strain rates. Predictions made using the presented methodology will be compared to experimental values and results obtained using the Generalized Method of Cells approach [2], a well-established micromechanics analysis method.

BACKGROUND

In a previous report [1], a detailed discussion of previous research in the areas of experimental determination of strain rate effects on composite material properties, rate dependent constitutive modeling of polymers and rate dependent constitutive modeling of polymer matrix composites was presented. Some of the key points of this review will be summarized here. Researchers such as Daniel, et. al. [3] determined experimentally that the material properties along the fiber direction of a carbon fiber reinforced polymer matrix composite showed little variation with strain rate. However, the transverse and shear moduli and strengths exhibited a significant variation with increasing strain rate. These results indicated that for these materials the deformation response is rate dependent, and the polymer matrix drives the rate dependence of the material properties.

To analyze the rate dependent deformation response of polymer matrix composites, both macroscopic and micromechanical techniques have been used. As an example of a macroscopic method, Weeks and Sun [4] developed a model in which a carbon fiber reinforced thermoplastic was considered to be an anisotropic, homogenous material. The behavior of an off-axis composite ply was modeled as a function of the fiber orientation angle. The inelasticity of the composite response was captured through the use of a quadratic plastic potential function, and the rate dependence of the material was simulated by making the material properties strain rate dependent. An example of a micromechanical technique is the work by Aidun and Addessio [5]. In this work, a nonlinear elastic polymer constitutive equation was implemented within the Method of Cells [6] micromechanics equations in order to compute the high strain rate response of a polymer matrix composite. Much of the remaining work in high strain rate constitutive modeling has assumed elastic, rate independent material behavior. As the actual material response is often rate dependent and nonlinear for high strain rate impact applications, there exists a significant need for further work in incorporating these types of behaviors into analytical models.

To predict the effective properties and response of a composite material using a micromechanics approach, several different methodologies have been utilized. These techniques have been thoroughly reviewed and discussed in works such as [6-10]. In general, three types of techniques are used. All of these approaches are based on analyzing the behavior of a unit cell of the composite. The unit cell is the smallest portion of the composite for which the behavior of the unit cell is considered to be representative of the response of the composite as a whole. The simplest types of techniques are mechanics of materials based methods, in which various uniform stress and uniform strain assumptions are utilized within the composite unit cell to compute the effective properties and response of the material. Examples of this type of approach include the traditional "rule of mixtures" equations [7], and the simplified micromechanics equations developed by Murthy and Chamis [11]. While this approach involves a great deal of approximation and simplification, the resulting equations are very simple in form, are very easy to implement within a computer code, and are very computationally efficient.

A more sophisticated method to compute the effective properties of composite materials involves utilizing continuum mechanics techniques. In this type of approach, the equations of continuum mechanics are solved in an average sense within the unit cell. Examples of this type of technique include the Concentric Cylinders Model [9], the Self Consistent Method [9], the Mori-Tanaka Method [12] and the Method of Cells [6]. Continuum mechanics methods more completely satisfy the field equations of mechanics, resulting in the physics of the problem being represented more accurately, than in mechanics of materials techniques. However, these approaches still often lend themselves to closed form solutions, which permit reasonable implementation and execution of these techniques within a computer code.

The most accurate and sophisticated micromechanics techniques are the numerically based methods. In this approach, the fiber and matrix are explicitly modeled using either finite elements or boundary elements. The effective response of the unit cell is then computed by conducting a finite element or boundary element analysis. Examples of this approach can be found in [13] and [14]. A numerical technique has also been developed by Walker, et. al. [15,16], in which integral equations are developed using Fourier series and Green's function approaches. The integral equations are then solved using numerical methods. This type of analysis yields the greatest accuracy, but the execution times required to conduct the analysis on a computer are often quite substantial. Analysis methods of this type will not be considered in this report, where only predicting the effective deformation response of a composite will be considered. Numerical techniques could prove useful in gaining insight into the detailed local stress states present in the composite unit cell. Examination of the detailed local stress states might be of assistance in the development of analytical strength and failure models.

MATRIX CONSTITUTIVE MODEL

The Ramaswamy-Stouffer viscoplastic state variable model [17], which was originally developed for metals, was modified to simulate the rate dependent inelastic response of the polymer matrix materials. As discussed in [1], there are sufficient similarities between the inelastic deformation response of metals and the inelastic response of polymers to permit the use of constitutive equations which were developed for metals to analyze polymers. It should be noted that the effects of hydrostatic stress states on the inelastic strains are currently being neglected. In the modified Ramaswamy-Stouffer model, the inelastic strain rate, $\dot{\varepsilon}_{ij}^{I}$, is defined as a function of the overstress, or difference between the deviatoric stress components, s_{ij}, and back stress state variable components, Ω_{ij}, in the form:

$$\dot{\varepsilon}_{ij}^{I} = D_o \exp\left[-\frac{1}{2}\left(\frac{Z_o^2}{3K_2}\right)^n\right] * \frac{s_{ij} - \Omega_{ij}}{\sqrt{K_2}} \tag{1}$$

where D_o, Z_o, and n are material constants, and K_2 is defined as follows:

$$K_2 = \frac{1}{2}\left(s_{ij} - \Omega_{ij}\right)\left(s_{ij} - \Omega_{ij}\right) \tag{2}$$

The elastic components of strain are added to the inelastic strain to obtain the total strain. The following relation defines the back stress variable rate:

$$\dot{\Omega}_{ij} = \frac{2}{3} q\Omega_m \dot{\varepsilon}_{ij} - q\Omega_{ij}\dot{\varepsilon}_e^{I} \tag{3}$$

where q is a material constant, Ω_m is a material constant which represents the maximum value of the back stress, and $\dot{\varepsilon}_e^I$ is the effective inelastic strain rate, defined as follows:

$$\dot{\varepsilon}_e^I = \sqrt{\frac{2}{3}\dot{\varepsilon}_{ij}\dot{\varepsilon}_{ij}} \tag{4}$$

where repeated indices indicate summation using the standard indicial notation definitions [17].

To obtain the material constants for this material model, the saturation stress values (the stress level where the stress-strain curve flattens out) from several constant strain rate tensile tests are utilized. In addition, the average inelastic strain at saturation is used. Equations (1)-(4) and linear regression techniques are then applied to obtain the material constants. More details on the constitutive equations and obtaining the material constants can be found in [1].

MICROMECHANICS MODEL

Overview

The effective properties and deformation response of the composite materials examined in this study were computed by using a micromechanics model. As mentioned previously, in micromechanics methods the effective properties and deformation response of a composite material unit cell are predicted based on the properties and response of the individual constituents. For this study, the composite unit cell will be defined as consisting of a single continuous fiber and its surrounding matrix. Only laminated composites will be analyzed; woven composites will not be considered at the present time. The matrix constituent and the composite as a whole will be assumed to have a sufficient degree of ductility such that the inelastic strain levels are significant.

The composites will be assumed to have a periodic, square, fiber packing arrangement, with perfect bonding between the fiber and the matrix These assumptions are common in the micromechanical analysis of composite materials [7-10]. While actual composites often have more complicated fiber architectures [18], for this preliminary study a periodic, square fiber packing was utilized in order to simplify the development of the micromechanics equations and to minimize the computational effort required. If future analytical results indicate that fiber packing plays a significant role in either the deformation or failure of polymer matrix composites under high strain rate loads, modifications to the micromechanical models could be made or selected detailed finite element analyses might be performed. In addition, the assumption of perfect bonding, a common assumption for polymer matrix composites, was made in order to simplify the development of the micromechanics equations. If fiber/matrix debonding turns out to play a significant role in the strength and failure analyses of the materials under consideration, appropriate modifications could be made to the equations.

Only unidirectional composites at various fiber orientation angles will be analyzed with the micromechanics techniques considered here. To model full laminated composites with varying fiber orientation through the thickness, the finite element method will be utilized. In such an analysis, a layer of elements will be used to model a single ply of the composite at a specified orientation angle. Multiple layers of elements will then be used to simulate the composite laminate. An analysis of this type will not be considered in the present study, but will be conducted at a future date.

As discussed in a previous report [1], some efforts have been made by previous researchers to utilize equations of state on the micromechanical level in modeling the high strain rate response of polymer matrix composites. Equations of state are utilized to model the effects of changing density on the hydrostatic stress state in the material. These equations are usually only required for very high strain rate loading conditions. The strain rates utilized in this study will be assumed to be low enough that equation of state considerations will not be required.

The deformation response of the polymer matrix materials utilized in the composites considered in this study will be simulated using the modified Ramaswamy-Stouffer constitutive equations described in the previous section. The fibers of the composite will be assumed to be linear elastic, with rate independent properties. Temperature effects will not be considered, and small strain conditions will be assumed. Further discussions of the reasons and consequences of these assumptions can be found in [1].

Micromechanics Equations Overview

The micromechanics method utilized in this study is based on a method proposed by Sun and Chen [19]. In this approach, the composite unit cell is broken up into three subcells. One subcell represents the fiber while the remaining two subcells represent the matrix. This approach is similar to the Method of Cells approach utilized by Aboudi [6]. However, in the Method of Cells a displacement field is assumed for each subcell, and the equations of continuity and equilibrium are utilized to solve for the subcell and effective displacements and stresses. In the Sun and Chen approach, on the other hand, uniform stress and uniform strain assumptions, in combination with the material constitutive equations, are utilized to solve for the stresses and strains for each subcell and for the overall composite. Furthermore, the Sun and Chen model was developed for a plane stress condition, and classical plasticity theory was utilized to account for any inelastic strains which might be present. In addition, the Sun and Chen model utilized a stress controlled loading condition, which is not particularly useful for finite element applications.

Robertson and Mall revised and expanded the Sun and Chen model [20-22]. In this technique, the plane stress assumption was removed, and the full three-dimensional stress and strain state was computed for each subcell and for the overall composite. Since the model is fully three-dimensional, four subcells are utilized to represent the unit cell. One subcell is used to represent the fiber, and the remaining three subcells represent the

surrounding matrix material. The Robertson and Mall model also utilized unified state variable constitutive equations to compute the inelastic strains in the matrix material. However, the equations are still designed to utilize stress controlled loading, in which the subcell stresses and strains are computed based on a defined effective stress condition. Since Robertson and Mall concentrated on analyzing metal matrix composites, where fiber/matrix debonding is significant, the equations were also modified to allow for the presence of a weak fiber/matrix interface. Pindera and Bednarcyk [23] utilized a similar approach in reformulating the Generalized Method of Cells [2]. In this work, the original equations of the Generalized Method of Cells were reformulated so that the subcell stresses are solved for in terms of the total strains and the subcell inelastic strains.

The micromechanics model utilized in this study is similar to that utilized by Robertson and Mall, in that uniform stress and uniform strain assumptions are applied to a four subcell unit cell, which is displayed in Figure 1. In this figure, subcell "Af" is the fiber subcell and subcells "Am", "B1", and "B2" are composed of matrix material. The material axis system is as shown in the figure. The "1" coordinate direction is along the fiber direction, while the "2" and "3" coordinate directions are perpendicular to the fiber. The fiber is idealized as having a square shape, with the side length equal to the square root of the fiber volume fraction. Assuming a square fiber shape will result in the interfacial stresses not being predicted correctly. However, due to the perfect bonding assumption, as well as the expected failure modes in the chosen application, the accurate prediction of interfacial stresses will be assumed to not be critical. The full three-dimensional stresses and strains are computed for each subcell and for the unit cell as a whole. By removing the plane stress assumption, thick composites can be analyzed. Furthermore, through the thickness stresses can be more accurately computed, which will most likely be important in modeling high strain rate impact normal to the plane of the laminate. In the model utilized in this study, strain controlled loading is assumed. The loading condition is the primary difference between this method and the Robertson and Mall technique. Utilization of strain controlled loading will simplify the implementation of this model into a finite element code. In a user defined material subroutine in a finite element code, strains are passed into the routine, and stresses are computed and passed back to the calling routines.

Micromechanics Equations Derivation

The unit cell utilized in the development of the micromechanics equations is shown in Figure 1. The bottom layer of subcells, with subcells "Af" and "Am", is referred to as region "A". The top layer of subcells, with subcells "B1" and "B2", is referred to as region "B". Region "A′" is defined as consisting of subcells "Af" and "B1", and region "B′" is defined as consisting of subcells "Am" and "B2". The subscript "f" will be used to denote fiber related properties, and the subscript "m" will be used to denote matrix related properties. Subscripts "Af", "Am", "B1" and "B2" will be used to denote stresses and strains of the individual subcells. Subscripts "A", "B", "A′", and "B′" will be used to denote stresses and strains in the corresponding regions as defined above. Stresses and strains with no region identifying subscript will be assumed to represent the total effective

stresses and strains for the unit cell. A superscript "I" will be used to denote inelastic strains. The subscripts "11", "22" and "33" will be used to define normal stresses, strains and material properties, with the coordinate directions as defined in Figure 1. The subscripts "12", "13" and "23" will be used to define shear stresses, strains, and material properties.

The symbol "E" represents the elastic modulus, the symbol "G" represents the shear modulus, and the symbol "ν" represents the Poisson's ratio. The symbol "σ_{ij}" represents stress tensor components, the symbol "ε_{ij}" represents strain tensor components, and the symbol "γ_{ij}" represents engineering shear strain components. The symbol "kf" represents the fiber volume ratio of the composite.

The stress and strain in each subcell are assumed to be the effective stress and strain, equal to the integral of the actual stress or strain over the volume of the subcell. These values are assumed to be uniform over the volume of the subcell. The effective stress and strain in region "A", region "B", region "A′" and region "B′" are defined as the volume average of the stresses and strains in the corresponding subcells. The effective stress and strain in the unit cell are defined as the volume average of the stresses and strains in region A and region B (or region A′ and region B′). To determine the volume average, a weighted sum is computed where the value (stress or strain) in each subcell or region is weighted by the ratio of the volume of the subcell (or region) over the total volume of the region (or unit cell).

The components in the transversely isotropic compliance matrix (the inverse of the stiffness matrix) for the fiber are defined as follows. Note that the symbol S_{ij}, which is used to denote the terms in the compliance matrix, is not to be confused with the symbol s_{ij}, which was used in Equations (1)-(4) to represent the components of deviatoric stress.

$$S_{11f} = \frac{1}{E_{11f}}, S_{22f} = \frac{1}{E_{22f}}, S_{12f} = \frac{-\nu_{12f}}{E_{11f}}, S_{23f} = \frac{-\nu_{23f}}{E_{22f}}, S_{44f} = \frac{1}{G_{23f}}, S_{66f} = \frac{1}{G_{12f}} \quad (5)$$

where, for example, E_{11f} represents the longitudinal elastic modulus of the fiber (along the 1 direction axis in Figure 1), ν_{12f} represents the axial Poisson's ratio of the fiber, and G_{12f} represents the in-plane shear modulus of the fiber.

The components of the compliance matrix for the isotropic matrix material are defined as follows:

$$S_{11m} = \frac{1}{E_m}, S_{12m} = \frac{-\nu_m}{E_m}, S_{66m} = \frac{1}{G_m} \quad (6)$$

where E_m represents the elastic modulus of the matrix, ν_m represents the Poisson's ratio of the matrix, and G_m represents the shear modulus of the matrix.

The transversely isotropic compliance matrix is utilized to relate the strains to the stresses, using the following relations:

$$\begin{Bmatrix} \varepsilon_{11} \\ \varepsilon_{22} \\ \varepsilon_{33} \end{Bmatrix} = \begin{bmatrix} S_{11} & S_{12} & S_{12} \\ S_{12} & S_{22} & S_{23} \\ S_{12} & S_{23} & S_{22} \end{bmatrix} \begin{Bmatrix} \sigma_{11} \\ \sigma_{22} \\ \sigma_{33} \end{Bmatrix} + \begin{Bmatrix} \varepsilon_{11}^{I} \\ \varepsilon_{22}^{I} \\ \varepsilon_{33}^{I} \end{Bmatrix} \tag{7}$$

$$\gamma_{12} = S_{66} * \sigma_{12} + 2 * \varepsilon_{12}^{I} \tag{8}$$

$$\gamma_{13} = S_{66} * \sigma_{13} + 2 * \varepsilon_{13}^{I} \tag{9}$$

$$\gamma_{23} = S_{44} * \sigma_{23} + 2 * \varepsilon_{23}^{I} \tag{10}$$

The addition of the inelastic strain components to the standard transversely isotropic elastic constitutive matrix is how the matrix inelasticity is incorporated into the constitutive relations. For the linearly elastic fiber, these components can be neglected. For the isotropic matrix, S_{23} is set equal to S_{12}, S_{22} is set equal to S_{11}, and S_{44} is set equal to S_{66}.

The effective total strain state in the composite unit cell is assumed to be given or computed before beginning the micromechanics computations. Furthermore, the inelastic strains in each subcell are assumed to be either known or estimated.

Normal Stresses and Strains

For the normal stresses and strains (11, 22 and 33), the following uniform stress and uniform strain assumptions are made:

$$\begin{aligned} \varepsilon_{11Af} &= \varepsilon_{11Am} = \varepsilon_{11A} \\ \varepsilon_{11B1} &= \varepsilon_{11B2} = \varepsilon_{11B} \\ \varepsilon_{11A} &= \varepsilon_{11B} = \varepsilon_{11} \end{aligned} \tag{11}$$

$$\begin{aligned} \sigma_{22Af} &= \sigma_{22Am} = \sigma_{22A} \\ \sigma_{22B1} &= \sigma_{22B2} = \sigma_{22B} \end{aligned} \tag{12}$$

$$\begin{aligned} \sigma_{33Af} &= \sigma_{33B1} = \sigma_{33A'} \\ \sigma_{33Am} &= \sigma_{33B2} = \sigma_{33B'} \end{aligned} \tag{13}$$

$$\varepsilon_{22A} = \varepsilon_{22B} = \varepsilon_{22} \tag{14}$$

$$\varepsilon_{33A'} = \varepsilon_{33B'} = \varepsilon_{33} \tag{15}$$

The effective stresses and strains in regions A, B, A′ and B′, as well as for the composite unit cell, are computed using volume averaging, yielding the following expressions:

$$\varepsilon_{22A} = \sqrt{kf} * \varepsilon_{22Af} + (1-\sqrt{kf}) * \varepsilon_{22Am} \tag{16}$$

$$\varepsilon_{22B} = \sqrt{kf} * \varepsilon_{22B1} + (1-\sqrt{kf}) * \varepsilon_{22B2} \tag{17}$$

$$\varepsilon_{33A'} = \sqrt{kf} * \varepsilon_{33Af} + (1-\sqrt{kf}) * \varepsilon_{33B1} \tag{18}$$

$$\varepsilon_{33B'} = \sqrt{kf} * \varepsilon_{33Am} + (1-\sqrt{kf}) * \varepsilon_{33B2} \tag{19}$$

$$\sigma_{11A} = \sqrt{kf} * \sigma_{11Af} + (1-\sqrt{kf}) * \sigma_{11Am} \tag{20}$$

$$\sigma_{11B} = \sqrt{kf} * \sigma_{11B1} + (1-\sqrt{kf}) * \sigma_{11B2} \tag{21}$$

$$\sigma_{11} = \sqrt{kf} * \sigma_{11A} + (1-\sqrt{kf}) * \sigma_{11B} \tag{22}$$

$$\sigma_{22} = \sqrt{kf} * \sigma_{22A} + (1-\sqrt{kf}) * \sigma_{22B} \tag{23}$$

$$\sigma_{33} = \sqrt{kf} * \sigma_{33A'} + (1-\sqrt{kf}) * \sigma_{33B'} \tag{24}$$

The constitutive relations for the fiber and matrix can be defined as follows, using the relations defined in Equation (7):

$$\varepsilon_{11f} = S_{11f} * \sigma_{11f} + S_{12f} * \sigma_{22f} + S_{12f} * \sigma_{33f} \tag{25}$$

$$\varepsilon_{22f} = S_{12f} * \sigma_{11f} + S_{22f} * \sigma_{22f} + S_{23f} * \sigma_{33f} \tag{26}$$

$$\varepsilon_{33f} = S_{12f} * \sigma_{11f} + S_{23f} * \sigma_{22f} + S_{22f} * \sigma_{33f} \tag{27}$$

$$\varepsilon_{11m} = S_{11m} * \sigma_{11m} + S_{12m} * \sigma_{22m} + S_{12m} * \sigma_{33m} + \varepsilon^{I}_{11m} \tag{28}$$

$$\varepsilon_{22m} = S_{12m} * \sigma_{11m} + S_{11m} * \sigma_{22m} + S_{12m} * \sigma_{33m} + \varepsilon^{I}_{22m} \tag{29}$$

$$\varepsilon_{33m} = S_{12m} * \sigma_{11m} + S_{12m} * \sigma_{22m} + S_{11m} * \sigma_{33m} + \varepsilon^{I}_{33m} \tag{30}$$

By solving Equations (25) and (28) for each subcell, and by utilizing the appropriate uniform stress and uniform strain assumptions, the following expressions are obtained. It

should be noted that the MATHCAD software package [24] was utilized to assist in carrying out the algebraic computations presented in this derivation.

$$\sigma_{11Af} = \frac{1}{S_{11f}}\left(\varepsilon_{11} - S_{12f} * \sigma_{22A} - S_{12f} * \sigma_{33A'}\right) \tag{31}$$

$$\sigma_{11Am} = \frac{1}{S_{11m}}\left(\varepsilon_{11} - S_{12m} * \sigma_{22A} - S_{12m} * \sigma_{33B'} - \varepsilon^{I}_{11Am}\right) \tag{32}$$

$$\sigma_{11B1} = \frac{1}{S_{11m}}\left(\varepsilon_{11} - S_{12m} * \sigma_{22B} - S_{12m} * \sigma_{33A'} - \varepsilon^{I}_{11B1}\right) \tag{33}$$

$$\sigma_{11B2} = \frac{1}{S_{11m}}\left(\varepsilon_{11} - S_{12m} * \sigma_{22B} - S_{12m} * \sigma_{33B'} - \varepsilon^{I}_{11B2}\right) \tag{34}$$

Equations (31)-(34) can then be substituted into Equations (26), (27), (29), and (30) for each subcell, applying the appropriate uniform stress and uniform strain assumptions. By substituting the resulting expressions into Equations (16)-(19), the following system of equations results:

$$\begin{aligned}
&\varepsilon_{22A} - \left(\sqrt{kf}\,\frac{S_{12f}}{S_{11f}} + (1-\sqrt{kf})\,\frac{S_{12m}}{S_{11m}}\right)\varepsilon_{11} + (1-\sqrt{kf})\,\frac{S_{12m}}{S_{11m}}\varepsilon^{I}_{11Am} \\
&-(1-\sqrt{kf})\,\varepsilon^{I}_{22Am} = \left(\sqrt{kf}\left(S_{22f} - \frac{S^2_{12f}}{S_{11f}}\right) + (1-\sqrt{kf})\left(S_{11m} - \frac{S^2_{12m}}{S_{11m}}\right)\right)\sigma_{22A} \\
&+\left(\sqrt{kf}\left(S_{23f} - \frac{S^2_{12f}}{S_{11f}}\right)\right)\sigma_{33A'} + \left((1-\sqrt{kf})\left(S_{12m} - \frac{S^2_{12m}}{S_{11m}}\right)\right)\sigma_{33B'}
\end{aligned} \tag{35}$$

$$\begin{aligned}
&\varepsilon_{22B} - \frac{S_{12m}}{S_{11m}}\varepsilon_{11} + \sqrt{kf}\,\frac{S_{12m}}{S_{11m}}\varepsilon^{I}_{11B1} - \sqrt{kf}\,\varepsilon^{I}_{22B1} + (1-\sqrt{kf})\,\frac{S_{12m}}{S_{11m}}\varepsilon^{I}_{11B2} \\
&-(1-\sqrt{kf})\,\varepsilon^{I}_{22B2} = \left(S_{11m} - \frac{S^2_{12m}}{S_{11m}}\right)\sigma_{22B} + \left(\sqrt{kf}\left(S_{12m} - \frac{S^2_{12m}}{S_{11m}}\right)\right)\sigma_{33A'} \\
&+\left((1-\sqrt{kf})\left(S_{12m} - \frac{S^2_{12m}}{S_{11m}}\right)\right)\sigma_{33B'}
\end{aligned} \tag{36}$$

$$\varepsilon_{33A'} - \left(\sqrt{kf}\frac{S_{12f}}{S_{11f}} + (1-\sqrt{kf})\frac{S_{12m}}{S_{11m}}\right)\varepsilon_{11} + (1-\sqrt{kf})\frac{S_{12m}}{S_{11m}}\varepsilon^{I}_{11B1}$$
$$-(1-\sqrt{kf})\varepsilon^{I}_{33B1} = \left(\sqrt{kf}\left(S_{22f} - \frac{S^2_{12f}}{S_{11f}}\right) + (1-\sqrt{kf})\left(S_{11m} - \frac{S^2_{12m}}{S_{11m}}\right)\right)\sigma_{33A'} \qquad (37)$$
$$+\left(\sqrt{kf}\left(S_{23f} - \frac{S^2_{12f}}{S_{11f}}\right)\right)\sigma_{22A} + \left(\left(1-\sqrt{kf}\right)\left(S_{12m} - \frac{S^2_{12m}}{S_{11m}}\right)\right)\sigma_{22B}$$

$$\varepsilon_{33B'} - \frac{S_{12m}}{S_{11m}}\varepsilon_{11} + \sqrt{kf}\frac{S_{12m}}{S_{11m}}\varepsilon^{I}_{11Am} - \sqrt{kf}\,\varepsilon^{I}_{33Am} + (1-\sqrt{kf})\frac{S_{12m}}{S_{11m}}\varepsilon^{I}_{11B2}$$
$$-(1-\sqrt{kf})\varepsilon^{I}_{33B2} = \left(S_{11m} - \frac{S^2_{12m}}{S_{11m}}\right)\sigma_{33B'} + \left(\sqrt{kf}\left(S_{12m} - \frac{S^2_{12m}}{S_{11m}}\right)\right)\sigma_{22A} \qquad (38)$$
$$+\left((1-\sqrt{kf})\left(S_{12m} - \frac{S^2_{12m}}{S_{11m}}\right)\right)\sigma_{22B}$$

Equations (35)-(38), together with Equations (31)-(34), can be solved for the required subcell stresses. Equations (12), (13), and (20)-(24) can then be used to solve for the effective stress state in the unit cell.

In-Plane Shear Stresses and Strains

For the in-plane shear (12) direction stresses and strains, the following uniform stress and uniform strain assumptions are made:

$$\gamma_{12A} = \gamma_{12B} = \gamma_{12} \qquad (39)$$

$$\sigma_{12Af} = \sigma_{12Am} = \sigma_{12A}$$
$$\sigma_{12B1} = \sigma_{12B2} = \sigma_{12B} \qquad (40)$$

By applying volume averaging, the effective in-plane shear stresses and strains in each region and for the composite unit cell are defined as follows:

$$\gamma_{12A} = \sqrt{kf} * \gamma_{12Af} + (1-\sqrt{kf}) * \gamma_{12Am}$$
$$\gamma_{12B} = \sqrt{kf} * \gamma_{12B1} + (1-\sqrt{kf}) * \gamma_{12B2} \qquad (41)$$

$$\sigma_{12} = \sqrt{kf} * \sigma_{12A} + (1-\sqrt{kf}) * \sigma_{12B} \qquad (42)$$

The constitutive relations for the fiber and matrix can be defined by the following expressions, using the relation defined in Equation (8):

$$\gamma_{12f} = S_{66f} * \sigma_{12f} \tag{43}$$

$$\gamma_{12m} = S_{66m} * \sigma_{12m} + 2 * \varepsilon^{I}_{12m} \tag{44}$$

By substituting Equations (43) and (44) into Equation (41), and using the appropriate uniform stress and uniform strain assumptions, the following expressions are obtained. These relations can be used to solve for the subcell in-plane shear stresses in region A and region B, and thus in the individual subcells:

$$\gamma_{12} = [\sqrt{kf} * S_{66f} + (1-\sqrt{kf}) * S_{66m}] * \sigma_{12A} + 2 * (1-\sqrt{kf}) * \varepsilon^{I}_{12Am} \tag{45}$$

$$\gamma_{12} = S_{66m} * \sigma_{12B} + 2 * \sqrt{kf} * \varepsilon^{I}_{12B1} + 2 * (1-\sqrt{kf}) * \varepsilon^{I}_{12B2} \tag{46}$$

Transverse Shear Stresses and Strains- (13) Direction

The computation of the subcell stresses in the (13) direction is very similar to the computation of the subcell stresses in the (12) direction, with the exception of using regions A′ and B′ instead of regions A and B. The uniform stress and uniform strain assumptions thus becoming the following:

$$\gamma_{13A'} = \gamma_{13B'} = \gamma_{13} \tag{47}$$

$$\begin{aligned} \sigma_{13Af} &= \sigma_{13B1} = \sigma_{13A'} \\ \sigma_{13Am} &= \sigma_{13B2} = \sigma_{13B'} \end{aligned} \tag{48}$$

The volume averaged stresses and strains in each region are computed using the expressions:

$$\begin{aligned} \gamma_{13A'} &= \sqrt{kf} * \gamma_{13Af} + (1-\sqrt{kf}) * \gamma_{13B1} \\ \gamma_{13B'} &= \sqrt{kf} * \gamma_{13Am} + (1-\sqrt{kf}) * \gamma_{13B2} \end{aligned} \tag{49}$$

$$\sigma_{13} = \sqrt{kf} * \sigma_{13A'} + (1-\sqrt{kf}) * \sigma_{13B'} \tag{50}$$

By substituting Equations (43) and (44) (replacing the subscript "12" with "13" as indicated by Equation (9)) into Equation (49), the transverse (13) shear stresses in the individual subcells can be computed from the following equations along with the uniform stress assumptions:

$$\gamma_{13} = [\sqrt{kf} * S_{66f} + (1-\sqrt{kf}) * S_{66m}] * \sigma_{13A'} + 2 * (1-\sqrt{kf}) * \varepsilon^{I}_{13B1} \tag{51}$$

$$\gamma_{13} = S_{66m} * \sigma_{13B'} + 2 * \sqrt{kf} * \varepsilon^{I}_{13Am} + 2 * (1 - \sqrt{kf}) * \varepsilon^{I}_{13B2} \tag{52}$$

Transverse Shear Stresses and Strains- (23) Direction

In computing the (23) direction subcell stresses and strains, the following uniform stress assumptions are made:

$$\sigma_{23A} = \sigma_{23B} = \sigma_{23} \tag{53}$$

$$\begin{aligned} \sigma_{23Af} &= \sigma_{23Am} = \sigma_{23A} \\ \sigma_{23B1} &= \sigma_{23B2} = \sigma_{23B} \end{aligned} \tag{54}$$

The volume averaged shear strains in each region are then defined as follows:

$$\begin{aligned} \gamma_{23A} &= \sqrt{kf} * \gamma_{23Af} + (1 - \sqrt{kf}) * \gamma_{23Am} \\ \gamma_{23B} &= \sqrt{kf} * \gamma_{23B1} + (1 - \sqrt{kf}) * \gamma_{23B2} \end{aligned} \tag{55}$$

$$\gamma_{23} = \sqrt{kf} * \gamma_{23A} + (1 - \sqrt{kf}) * \gamma_{23B} \tag{56}$$

The constitutive relations for the fiber and matrix are defined by using Equation (10):

$$\gamma_{23f} = S_{44f} * \sigma_{23f} \tag{57}$$

$$\gamma_{23m} = S_{66m} * \sigma_{23m} + 2 * \varepsilon^{I}_{23m} \tag{58}$$

By substituting Equations (57) and (58) into Equations (55) and (56), and by using the uniform stress assumptions, the following expression is obtained which can be used to compute the subcell transverse (23) direction shear stresses:

$$\begin{aligned} \gamma_{23} &= [kf * S_{44f} + (1 - kf) * S_{66m}] * \sigma_{23} \\ &+ 2 * (1 - \sqrt{kf}) * [\sqrt{kf} * (\varepsilon^{I}_{23Am} + \varepsilon^{I}_{23B1}) + (1 - \sqrt{kf}) * \varepsilon^{I}_{23B2}] \end{aligned} \tag{59}$$

Numerical Implementation of Micromechanics Equations

For the current study, a stand-alone computer code was developed in order to implement and test the micromechanics equations. A standard fourth order Runge-Kutta explicit integration scheme [25] was utilized to integrate the rate dependent constitutive equations. Implicit integration algorithms are more numerically stable than explicit integration techniques, and were utilized in the original development of the matrix constitutive equations. However, the micromechanics algorithm will most likely eventually be implemented into a transient dynamic finite element code, which uses

explicit integration techniques. Therefore, the current algorithm was developed using an explicit integration scheme in order to assure compatibility. The Runge-Kutta method was employed for this preliminary study due to its simplicity and ease of implementation. Future efforts might include investigating more robust numerical techniques such as semi-implicit algorithms, which provide the stability of implicit methods while still maintaining the appearance of an explicit technique.

As mentioned in the development of the equations, strain controlled loading is assumed in the micromechanics algorithm. Strains are specified in a particular coordinate direction. To impose the required Poisson and axial-shear coupling strains, effective elastic properties for the composite at a specified fiber orientation angle are utilized. To compute the required elastic constants, the elastic constants in the material axis system are computed using equations developed by Murthy and Chamis [11]. The elastic constants in the structural axis system are then computed using standard techniques and equations described in references such as [7], [10] and [26]. The material axis system is the coordinate system shown in Figure 1. The structural axis system is the axis system along which the loads are applied. The material coordinate system is obtained by rotating the structural axis system about the "3" coordinate axis by an amount equal to the fiber orientation angle.

For the code execution, first the required geometric data (fiber volume ratio and fiber orientation angle), constituent properties and load history data are read in from an input file. The required elastic constants in both material and structural coordinate systems are computed, along with the required tensor transformation matrices. For each time step, the total strain rate in the load direction is computed. The Runge-Kutta integration procedure is then carried out to compute the total strain state in the structural axis system, as well as the inelastic strain and back stress value in each subcell. The total stresses in structural coordinates are then computed using the total strains, appropriate tensor transformations, and the micromechanics equations. The calculations for the next time step are then executed.

The Runge-Kutta integration algorithm involves the computation of several intermediate estimates of the total strain, subcell inelastic strain and subcell back stress. To compute the intermediate estimates, first the total strain estimate is converted from the structural axis system to the material axis system. The stresses in each of the subcells are then computed using the micromechanics equations. Using the computed stresses, the inelastic strain rate and back stress rate in each matrix subcell are computed using the matrix constitutive equations. The effective inelastic strain rate tensor for the composite unit cell is computed using a volume averaging technique in the material axis system, and the values are then transformed into the structural axis system. Using the computed effective Poisson's ratios and axial-shear coupling coefficients, the total strain rate tensor in structural coordinates is computed. The intermediate values required for the Runge-Kutta integration routine can then be determined.

VERIFICATION ANALYSES

Material Properties

To verify the micromechanics equations, a series of analyses were carried out using two material systems. Both material systems exhibit a nonlinear deformation response for off-axis fiber orientation angles. The first material system, supplied by Fiberite, Inc., consists of carbon IM-7 fibers in a 977-2 toughened epoxy matrix. Unidirectional laminates with fiber orientations of [0], [10], [45], and [90] were obtained. Tensile tests were conducted by Cincinnati Testing Labs of Cincinnati, Ohio at a strain rate of 1E-04 /sec on each of the composites [27]. Tensile and compressive tests at higher strain rates were also conducted at different labs, but the results are currently questionable and therefore will not be included here for verification purposes. While the developed methodology will eventually be applied to high strain rate impact applications, the current verification studies will only be carried out for relatively low strain rates. The analysis model, however, should be applicable to both low and high strain rate analyses.

The IM7/977-2 composite has a fiber volume ratio of 0.60. The IM-7 fibers have a longitudinal modulus of 276 GPa, a transverse modulus of 13.8 GPa, a Poisson's ratio of 0.25, and an in-plane shear modulus of 20.0 GPa [28]. The elastic modulus of the Fiberite 977-2 toughened epoxy is 3.65 GPa, and the Poisson's ratio is 0.40 [1]. The inelastic properties for the Fiberite 977-2 matrix, required for the modified Ramaswamy-Stouffer constitutive equations, are as follows for low strain rate tensile loading [1]: D_o=1E+04 /sec, n=0.50, Z_o=1030 MPa, q=160, Ω_m=69 MPa.

The second material that was studied consists of carbon AS4 fibers in a PEEK thermoplastic matrix. This material system was considered due to the fact that the PEEK thermoplastic is more ductile than the Fiberite 977-2 epoxy. Therefore, as discussed in more detail in [1], fewer approximations were required in order to determine the inelastic material constants for the PEEK material. As a result, the predictive capabilities of the micromechanics equations could be more accurately evaluated. Tensile stress-strain curves were obtained by Weeks and Sun [4] for unidirectional composites with fiber orientations of [14], [30], [45] and [90] at a strain rate of 1E-05 /sec, and composites with fiber orientations of [15], [30], [45] and [90] at a strain rate of 0.1 /sec.

The fiber volume ratio used for the AS4/PEEK material was 0.62 (a typical value for this material based on representative manufacturer information). The longitudinal modulus of the AS-4 fibers is 214 GPa, the transverse modulus is 14 GPa, the Poisson's ratio is 0.2, and the in-plane shear modulus is 14 GPa [29]. For the PEEK matrix, the elastic modulus is 4000 MPa and the Poisson's ratio is 0.40 [1]. The inelastic material constants for the modified Ramaswamy-Stouffer constitutive equations were determined in [1] and are as follows: D_o=1E+04 /sec, n=0.46, Z_o=630 MPa, q=310, Ω_m=52 MPa.

Analysis Results

The results predicted using the developed micromechanics equations (referred to as the mechanics of materials method in the following discussion) are compared both to experimental results and results obtained using the Generalized Method of Cells (GMC), a well-established micromechanics analysis method [2]. In GMC, the composite unit cell is divided into an arbitrary number of subcells. For the current study, a four subcell model was used, in order to make the unit cells for the two analysis methods consistent. In GMC, the displacement field in each subcell is approximated using a first order Taylor series expansion. The average stress and strain rates in each subcell are then defined in terms of the assumed displacement field. Displacement and traction continuity is then defined between the boundaries of the subcells and between adjoining unit cells. A system of equations then results which describes the combined elastic and inelastic response of the composite based on the geometry and properties of the individual constituents. To compute the response of composites at off-axis fiber orientation angles, classical lamination theory is used. In the lamination theory, the unit cell is assumed to be under a state of plane stress. GMC is currently implemented within a computer code entitled MAC (Micromechanics Analysis Code). Version 2.0 of MAC was used to conduct the analyses shown in this study [30].

The stress-strain curves obtained for the IM7/977-2 laminates are shown in Figures 2-5. For all of the analyses, 1000 time steps were used. In each of the figures, the results computed using the developed micromechanics equations (labeled Mech. Mat.) are compared to experimental values and results computed using the Generalized Method of Cells (labeled GMC). As can be seen in the figures, for the [0] and [90] fiber orientations the analysis results from the two micromechanics methods are almost identical, and both sets of computed results compare very well to the experimentally obtained values.

For the [10] and [45] fiber orientations, the results predicted by the two micromechanics methods are identical over the elastic portions of the response. GMC, however, predicts a softer response in the inelastic portion of the stress-strain curve than the mechanics of materials approach. For the [10] fiber orientation, the mechanics of materials approach predicts both the shape of the stress-strain curve and the numerical stress values much better than GMC. For the [45] fiber orientation, while both micromechanics methods predict stress values that compare reasonably well to the experimental values, the mechanics of materials results more accurately capture the shape of the stress-strain curve. The reasons for the softer response predicted by GMC are currently not well understood. The plane stress assumptions used in the GMC laminate theory may result in an overly high stress state being predicted in the matrix, which would result in the softer inelastic response. However, the comparisons seen between the present micromechanics method and GMC are similar to the comparisons between the Robertson and Mall model and the Method of Cells [21,22], which indicates that the current results are at least consistent.

Stress-strain results computed for the AS4/PEEK composite are shown in Figures 6-9 for a strain rate of 1E-05 /sec, and in Figures 10-13 for a strain rate of 0.1 /sec. The results computed using the developed micromechanics equations are once again compared both to experimental values and results computed using GMC. As can be seen in the figures, the trends in the results are very similar to those observed for the IM7/977-2 composite. However, the general comparison between the computed and experimental results is much better for the AS4/PEEK composite than for the IM7/977-2 system, particularly for the lower fiber orientation angles. The reason for this improvement may be related to the fact that, as discussed in [1], fewer approximations were required in determining the inelastic material constants for the PEEK thermoplastic than for the Fiberite 977-2 epoxy. The results computed for the lower strain rate compare somewhat better to the experimental values that the values computed at the higher strain rate. The cause for this improvement may be related to the fact that the strain rate of 0.1 /sec is somewhat above the strain rate level at which the PEEK material was characterized. Therefore, the nonlinear deformation response of PEEK at the higher strain rate may be somewhat different that that predicted by the derived inelastic material constants.

To demonstrate the ability of the micromechanics equations to capture the rate dependence of the composite response, computed and experimental results for the AS4/PEEK laminate with a [45] fiber orientation are shown in Figure 14. Results obtained at strain rates of 1E-05 /sec and 0.1 /sec are displayed. As can be seen in the figure, at the higher strain rate both the experimental and computed stress-strain curves exhibit higher stress levels and less nonlinearity when compared to the results obtained at the lower strain rate. While the differences between the results at the two different strain rates are not particularly dramatic, they are noticeable. The results obtained at much higher strain rates, on the order of several hundred per second, would most likely show an even more significant variation from these results obtained at relatively low strain rates. The important point to note from this figure is that the deformation response does vary with strain rate, and the micromechanics equations do capture the rate dependence of the material.

The deformation response of a polymer matrix composite also varies with fiber orientation angle. Results computed using the developed micromechanics equations for the AS4/PEEK composite at a strain rate of 1E-05 /sec are shown in Figure 15 for a variety of fiber orientations. As the fiber orientation angle is increased from more fiber dominated orientations (such as [14]) to more matrix dominated orientations (such as [45] or [90]), the predicted stress levels decrease dramatically. These results are what are expected for a continuous fiber reinforced unidirectional composite, which indicates that the micromechanics equations are capturing this effect correctly.

Overall, the deformation response predicted by the developed micromechanics equations compares reasonably well to the experimental results for both material systems studied. Furthermore, the predictions are reasonably good over a range of fiber orientation angles and strain rates. As seen in the predictions for the AS4/PEEK material, the rate dependence of the material response is captured by the micromechanics predictions.

The results predicted using the micromechanics equations developed here also compare well to the results predicted using the Generalized Method of Cells, and are at least as accurate when compared to experimental values. In addition, the developed micromechanics technique is very computationally efficient. Each of the analyses presented here used less than five seconds of CPU time on a Sun SPARC 5 workstation . Furthermore, the computer code for implementing the current micromechanics equations is very compact, which will most likely simplify the implementation of the method into a finite element code.

CONCLUSIONS

In this study, a set of micromechanics equations based on constant stress and constant strain assumptions have been developed to predict the inelastic, rate dependent response of polymer matrix composites. A unified state variable model based on the Ramaswamy-Stouffer constitutive equations developed for metals is utilized to compute the inelastic response of the polymer matrix. The stress-strain deformation response of two representative polymer matrix composites was predicted for several fiber orientation angles and strain rates. The results predicted using the micromechanics equations compared well both to experimentally obtained values and the results predicted using an alternative micromechanics analysis method. The results indicate that the current micromechanics model provides an accurate, efficient methodology for predicting the inelastic rate dependent response of polymer matrix composites.

Future work will involve developing a damage and failure model, based on local failure mechanisms, which will be implemented within the micromechanics equations. The combined deformation and failure model will then be implemented into a transient dynamic finite element code. Full deformation and failure analyses will then be conducted for a high strain rate impact problem such as simulating a split Hopkinson bar experiment on a composite specimen. Ultimately, the developed methodology will be used to simulate the response of composite structures subject to a high strain rate impact.

REFERENCES

1. Goldberg, R.K.; and Stouffer, D.C.: High Strain Rate Deformation Modeling of a Polymer Matrix Composite: Part I-Matrix Constitutive Equations. NASA TM-206969, 1998.

2. Paley, M.; and Aboudi, J.: Micromechanical Analysis of Composites by the Generalized Method of Cells Model. Mechanics of Materials, Vol 14, pp. 127-139, 1992.

3. Daniel, I.M.; Hamilton, W.G.; and LaBedz, R.H.: Strain Rate Characterization of Unidirectional Graphite/Epoxy Composite. Composite Materials: Testing and Design (Sixth Conference), ASTM STP 787, I.M. Daniel, ed., American Society of Testing and Materials, pp. 393-413, 1982.

4. Weeks, C.A.; and Sun, C.T.: Nonlinear Rate Dependence of Thick-Section Composite Laminates. High Strain Rate Effects on Polymer, Metal and Ceramic Matrix Composites and

Other Advanced Materials, AD-Vol. 48, Y.D.S. Rajapakse and J.R. Vinson, eds., ASME, pp. 81-95, 1995.

5. Aidun, J.R.; and Addessio, F.L.: An Enhanced Cell Model with Nonlinear Elasticity. J. Comp. Mat, Vol. 30, pp. 248-280, 1996.

6. Aboudi, J.: Mechanics of Composite Materials: A Unified Micromechanical Approach. Elsevier, New York, 1991.

7. Agarwal, B.D.; and Broutman, L.J.: Analysis and Performance of Fiber Composites. John Wiley and Sons, New York, 1990.

8. Gibson, R.F.: Principles of Composite Material Mechanics., Mc-Graw Hill, New York, 1994.

9. Christensen, R.M.: Mechanics of Composite Materials. John Wiley & Sons, New York, 1979.

10. Hyer, M.W.: Stress Analysis of Fiber-Reinforced Composite Materials. Mc-Graw Hill, New York, 1998.

11. Murthy, P.L.N.; and Chamis, C.C.: Integrated Composite Analyzer (ICAN): Users and Programmers Manual. NASA TP-2515, National Aeronautics and Space Administration, 1986.

12. Benveniste, Y.: A New Approach to the Application of Mori-Tanaka's Theory in Composite Materials. Mech. Mater., Vol. 6, pp. 147-157, 1987.

13. Goldberg, R.K.; and Hopkins, D.A.: Application of the Boundary Element Method to the Micromechanical Analysis of Composite Materials. Comp. & Struct., Vol. 56, pp. 721-731, 1995.

14. Lerch, B.A.; Melis, M.E.; and Tong, M.: Experimental and Analytical Analysis of Stress-Strain Behavior in a $[90°/0°]_{2s}$ SiC/Ti-15-3 Laminate. NASA TM-104470, National Aeronautics and Space Administration, 1991.

15. Walker, K.P.; Jordan, E.H.; and Freed, A.D.: Equivalence of Green's Function and the Fourier Series Representation of Composites with Periodic Microstructure. Micromechanics and Inhomogeneity-The Toshira Mura 65^{th} Anniversary Volume, G.J. Weng, M. Taya and H. Abé, eds., Springer, New York, pp. 535-558, 1990.

16. Walker, K.P.; Freed, A.D.; and Jordan, E.H.: Microstress Analysis of Periodic Composite. Composites Engineering, Vol. 1, pp. 29-40, 1991.

17. Stouffer, D.C.; and Dame, L.T.: Inelastic Deformation of Metals. Models, Mechanical Properties and Metallurgy. John Wiley and Sons, New York, 1996.

18. Arnold, S.M.; Pindera, M.-J.; and Wilt, T.E.: Influence of Fiber Architecture on the Elastic and Inelastic Response of Metal Matrix Composites. NASA TM-106705. National Aeronautics and Space Administration, 1995.

19. Sun, C.T.; and Chen, J.-L.: A Micromechanical Model for Plastic Behavior of Fiber Composites. Comp. Sci. & Tech., Vol. 40, pp. 115-129, 1991.

20. Robertson, D.D.; and Mall, S.: Micromechanical Relations for Fiber-Reinforced Composites Using the Free Transverse Shear Approach. Journal of Composites Technology and Research, Vol. 15, pp. 181-192, 1993.

21. Robertson, D.D.; and Mall, S.: Micromechanical Analysis for Thermoviscoplastic Behavior of Unidirectional Fiber Composites. Comp. Sci. & Tech., Vol. 50, pp. 483-496, 1994.

22. Robertson, D.D.: and Mall, S.: A Non-Linear Micromechanics-Based Analysis of Metal-Matrix Composite Laminates. Comp. Sci. & Tech., Vol. 52, pp. 319-331, 1994.

23. Pindera, M.-J.; and Bednarcyk, B.A.: An Efficient Implementation of the GMC Micromechanics Model for Multi-Phased Materials with Complex Microstructures. NASA CR-202350, 1997.

24. MATHCAD, Version 6.0, User's Guide, MathSoft, Inc., 1995.

25. Kreyszig, E.: Advanced Engineering Mathematics, 7th Edition. John Wiley and Sons, New York, 1992.

26. Herakovich, C.T.: Mechanics of Fibrous Composites. John Wiley and Sons, New York, 1998.

27. Gieseke, B.: Private Communication, Cincinnati Testing Laboratories, Inc., 1997.

28. Gates, T.S.; Chen, J.-L.; and Sun, C.T.: Micromechanical Characterization of Nonlinear Behavior of Advanced Polymer Matrix Composites. Composite Materials: Testing and Design (Twelfth Volume), ASTM STP 1274, R.B. Deo and C.R. Saff, eds., American Society of Testing and Materials, pp. 295-319, 1996.

29. Murthy, P.L.N.; Ginty, C.A.; and Sanfeliz, J.G.: Second Generation Integrated Composite Analyzer (ICAN) Computer Code. NASA TP-3290, National Aeronautics and Space Administration, 1993.

30. Wilt, T.E.; and Arnold, S.M.: Micromechanics Analysis Code (MAC) User Guide: Version 2.0. NASA TM-107290, National Aeronautics and Space Administration, 1996.

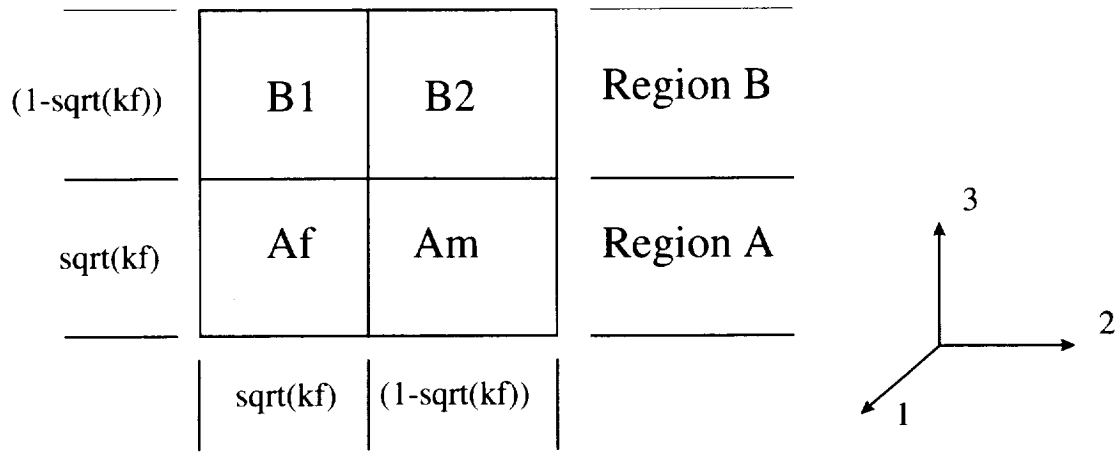

kf=Fiber Volume Fraction
Af=Fiber Subregion
Am, B1, B2=Matrix Subregions

Figure 1: Geometry and Layout of Mechanics of Materials Unit Cell Model.

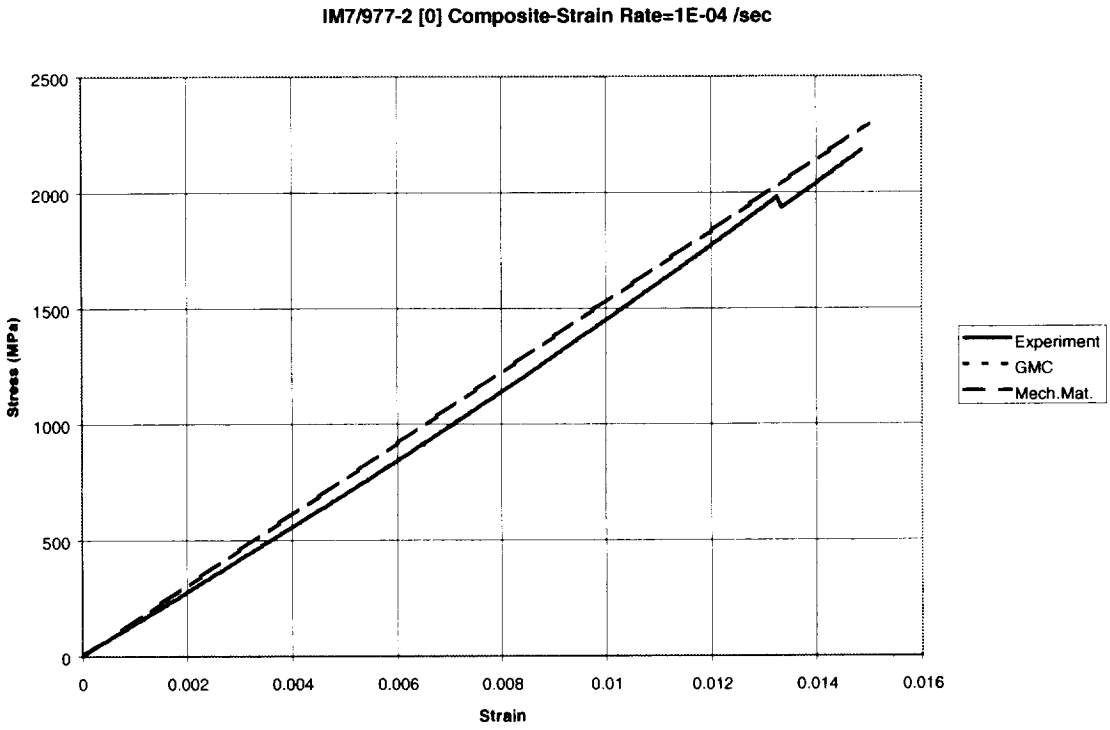

Figure 2: Model Predictions for IM7/977-2 [0] Laminate

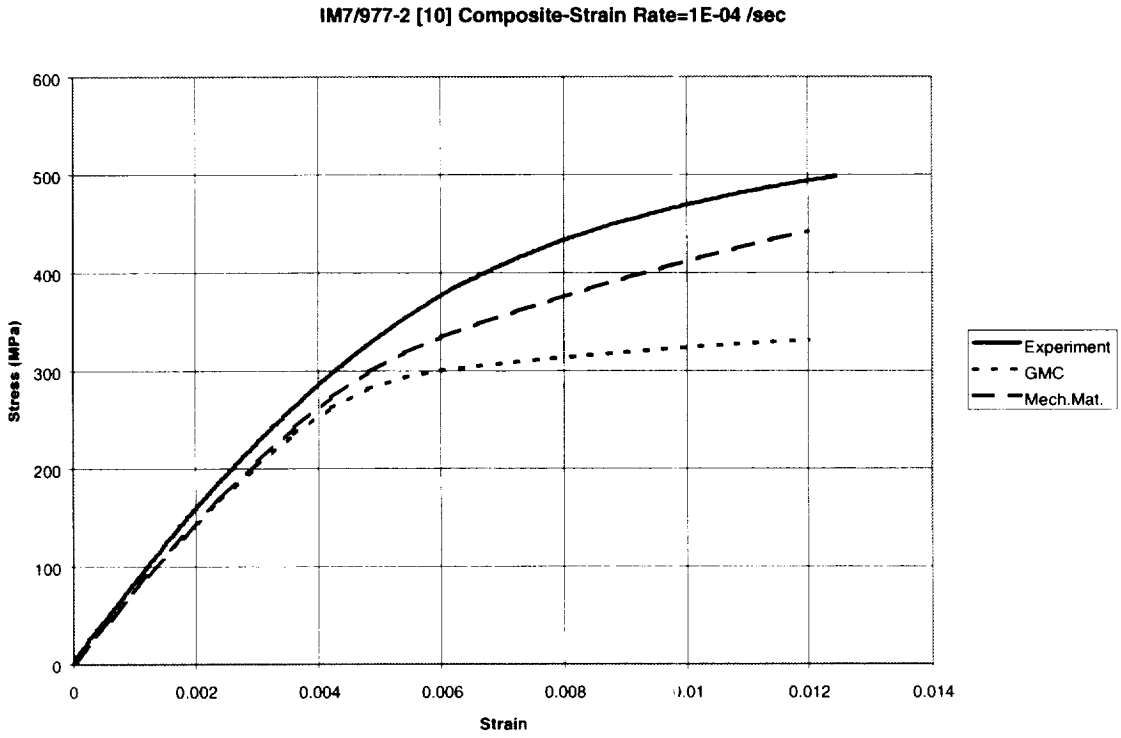

Figure 3: Model Predictions for IM7/977-2 [10] Laminate

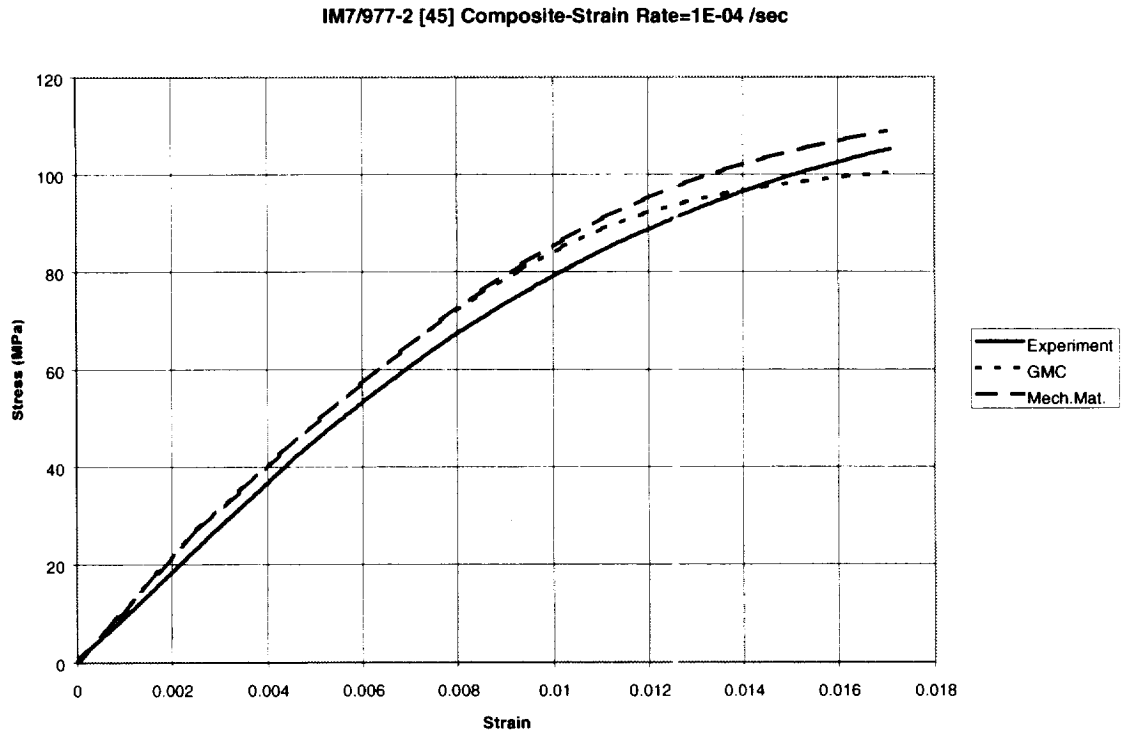

Figure 4: Model Predictions for IM7/977-2 [45] Laminate

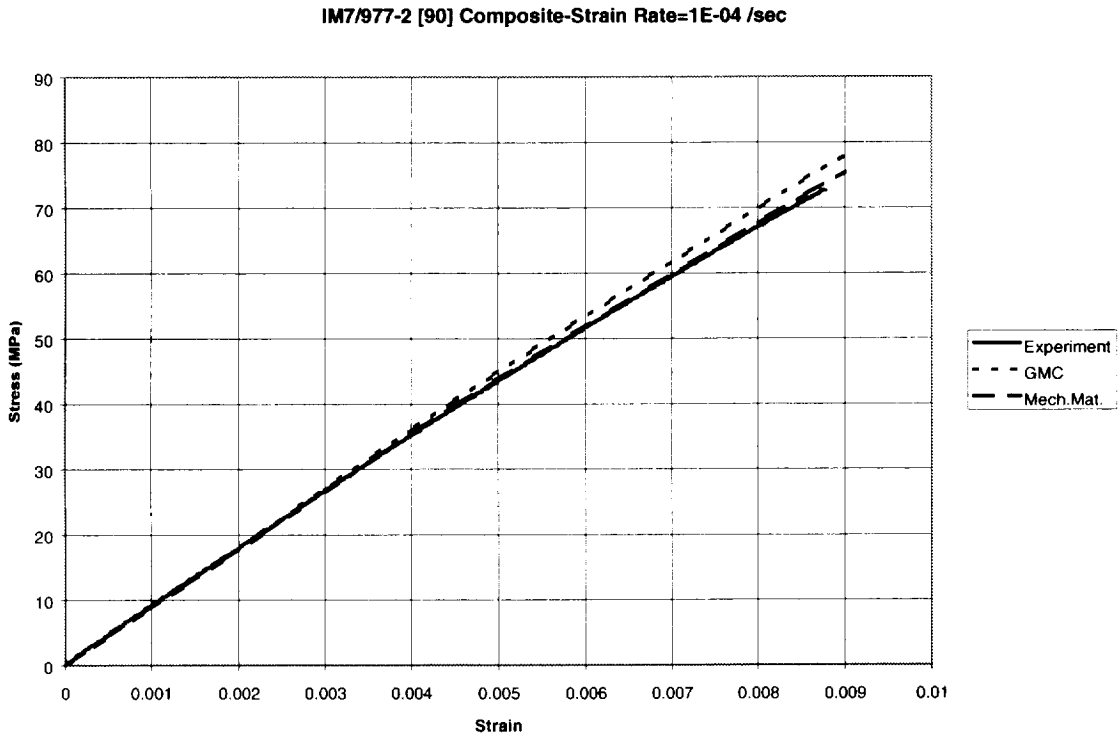

Figure 5: Model Predictions for IM7/977-2 [90] Laminate

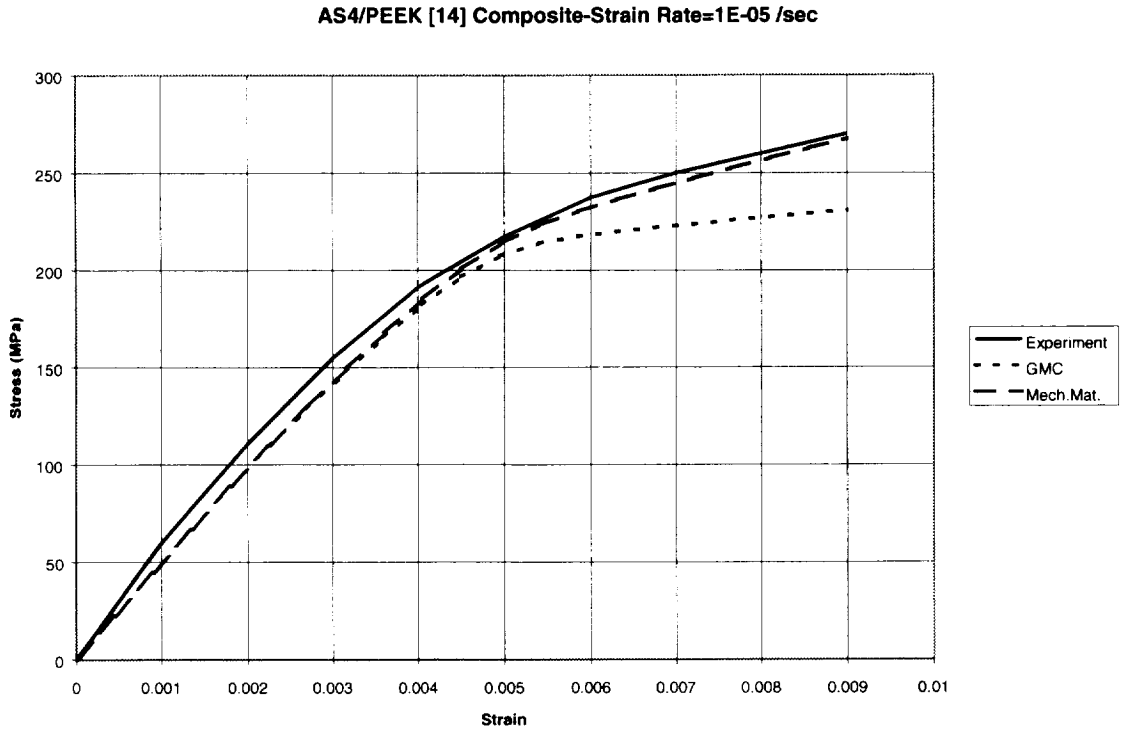

Figure 6: Model Predictions for AS4/PEEK [14] Laminate-Strain Rate=1E-05 /sec

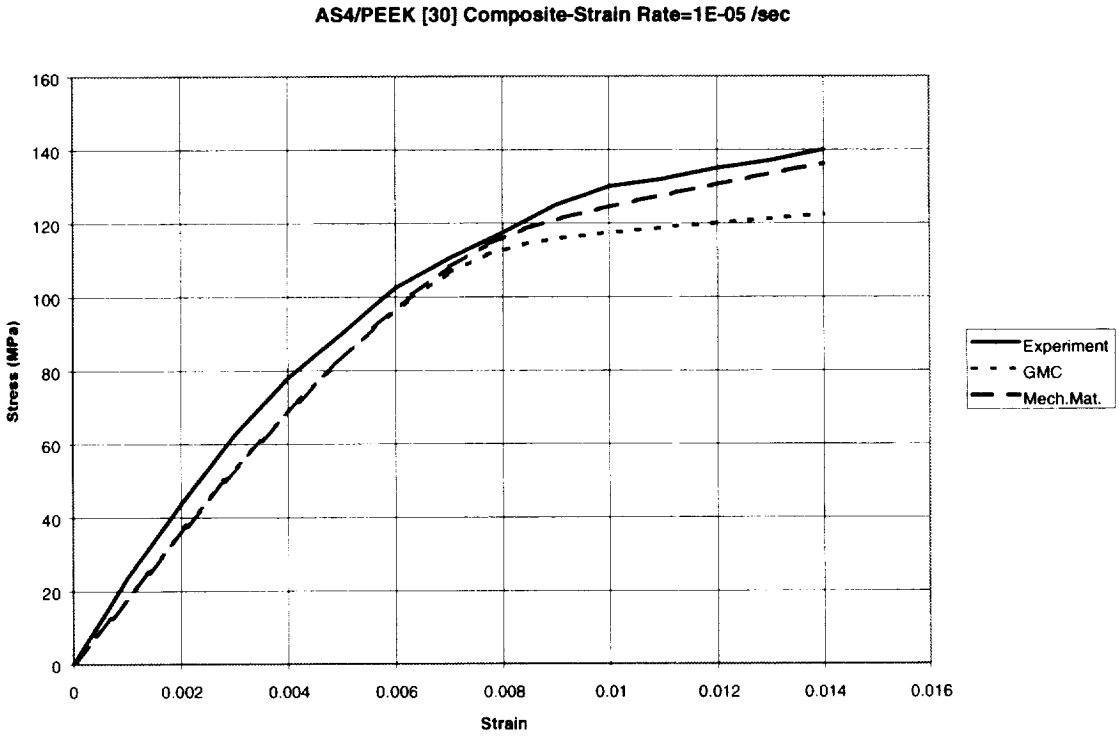

Figure 7: Model Predictions for AS4/PEEK [30] Laminate-Strain Rate=1E-05 /sec

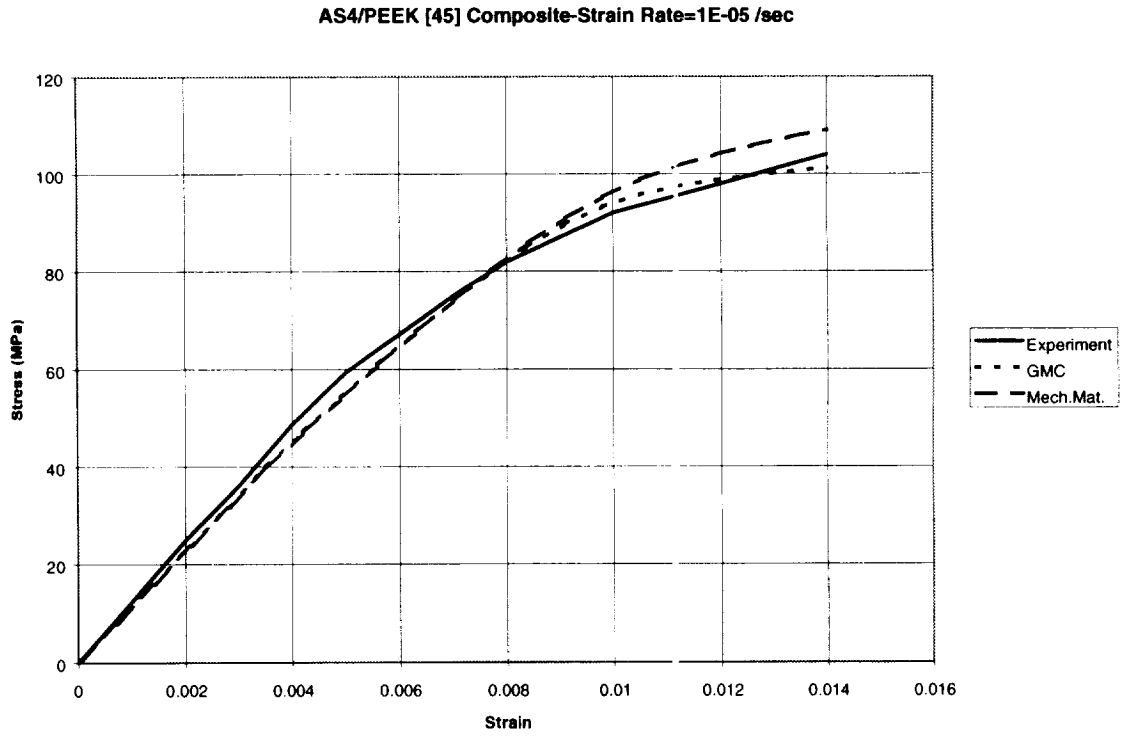

Figure 8: Model Predictions for AS4/PEEK [45] Laminate-Strain Rate=1E-05 /sec

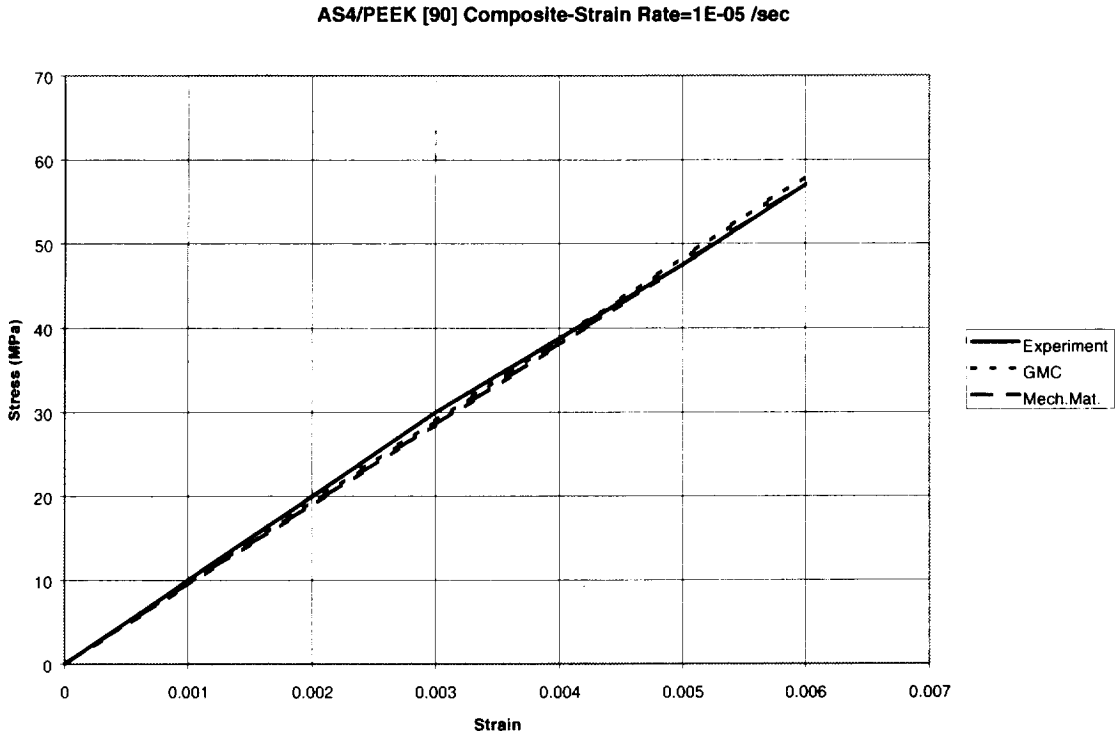

Figure 9: Model Predictions for AS4/PEEK [90] Laminate-Strain Rate=1E-05 /sec

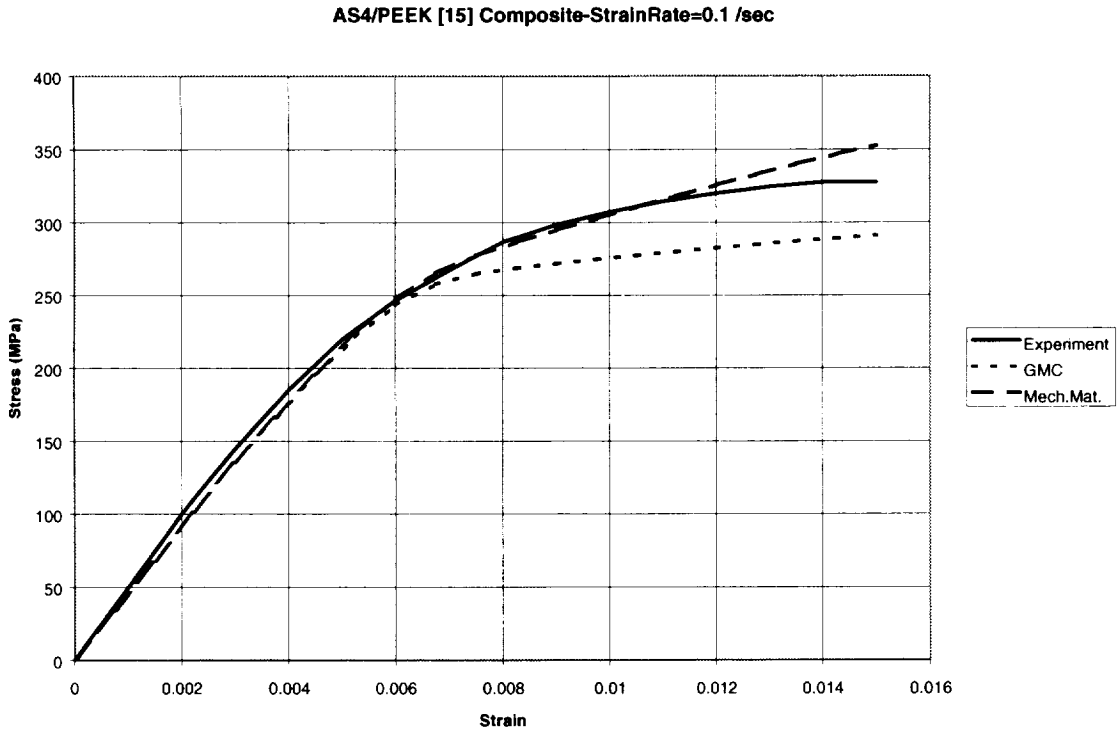

Figure 10: Model Predictions for AS4/PEEK [15] Laminate-Strain Rate=0.1 /sec

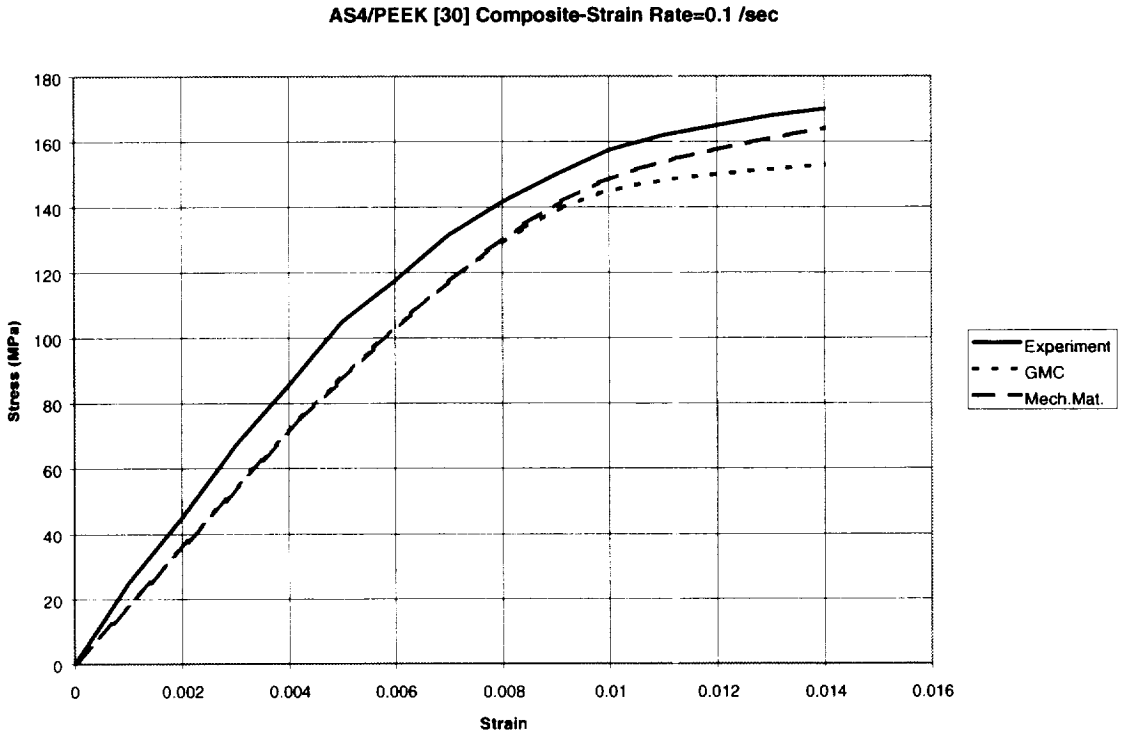

Figure 11: Model Predictions for AS4/PEEK [30] Laminate-Strain Rate=0.1 /sec

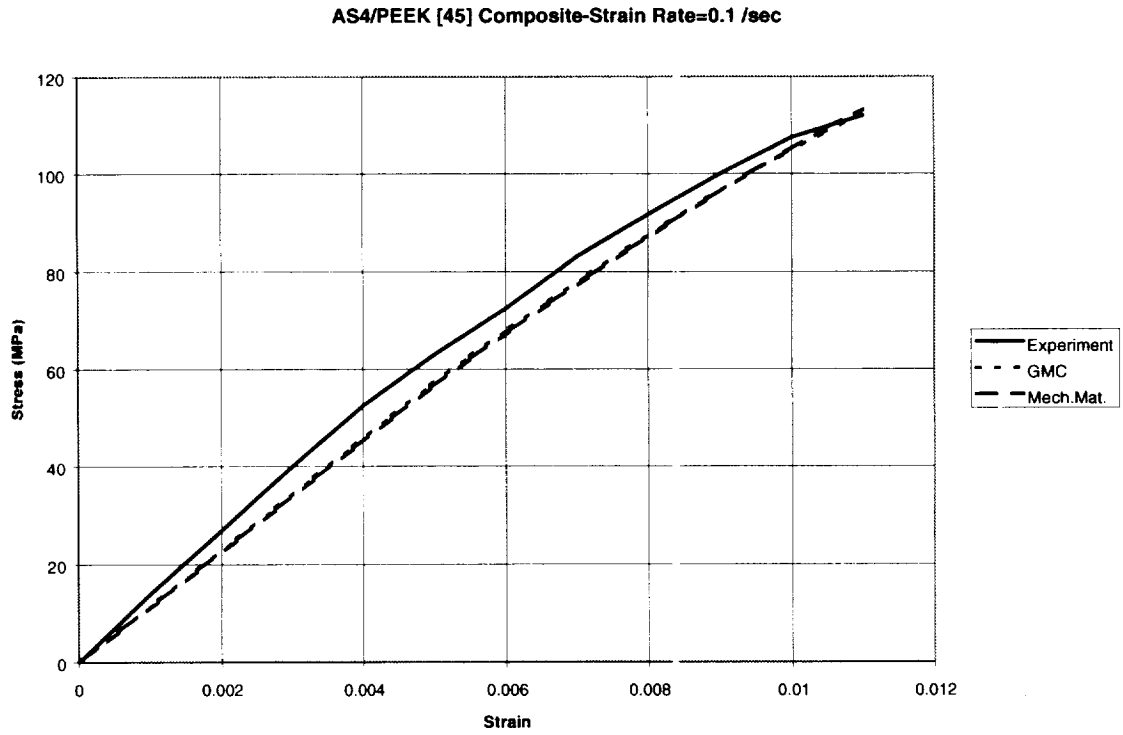

Figure 12: Model Predictions for AS4/PEEK [45] Laminate-Strain Rate=0.1 /sec

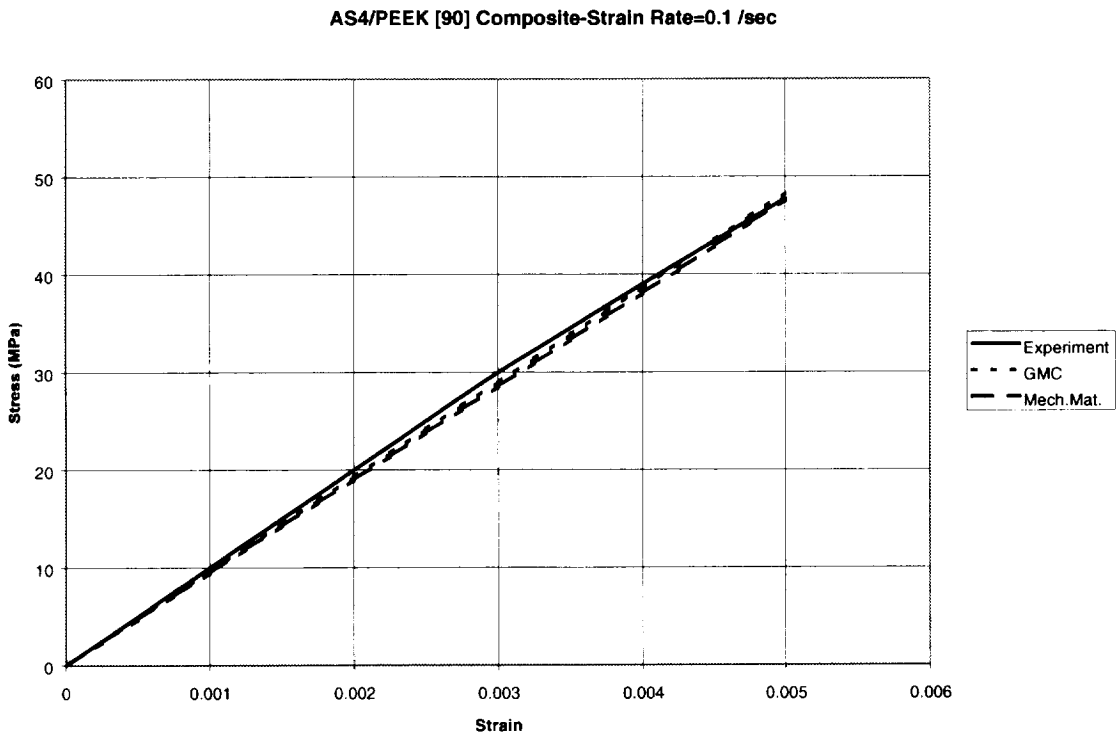

Figure 13: Model Predictions for AS4/PEEK [90] Laminate-Strain Rate=0.1 /sec

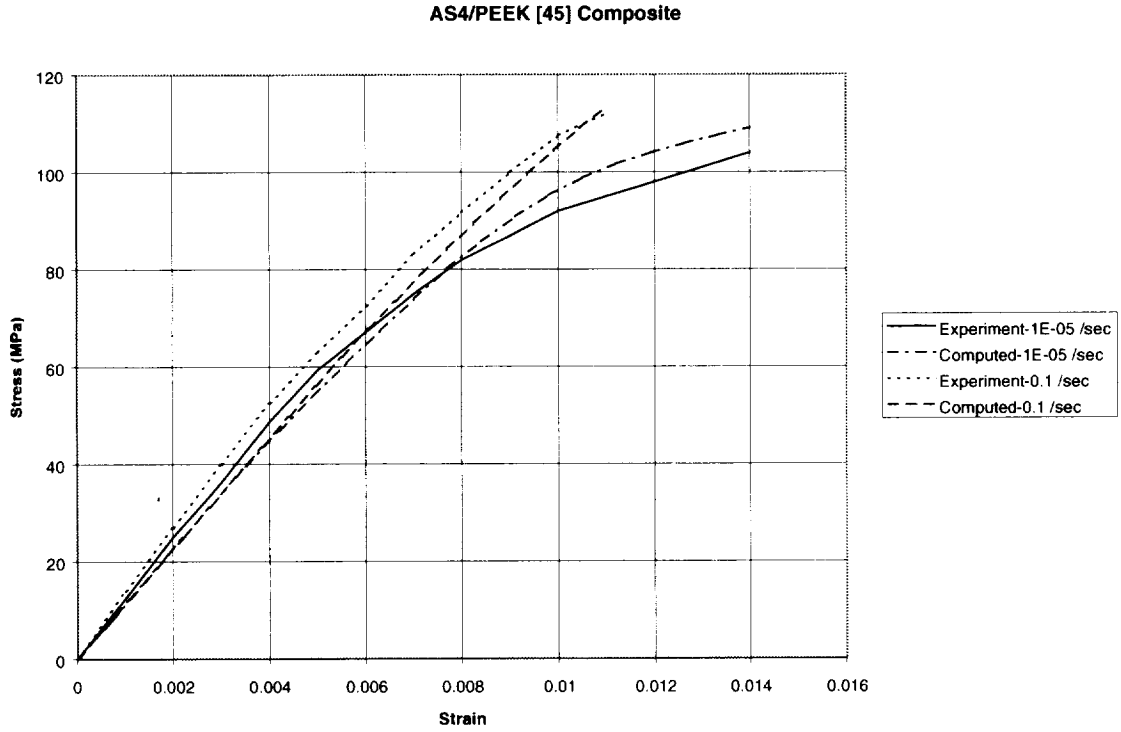

Figure 14: Model Predictions of Strain Rate Dependence of Deformation Response for AS4/PEEK [45] Laminate

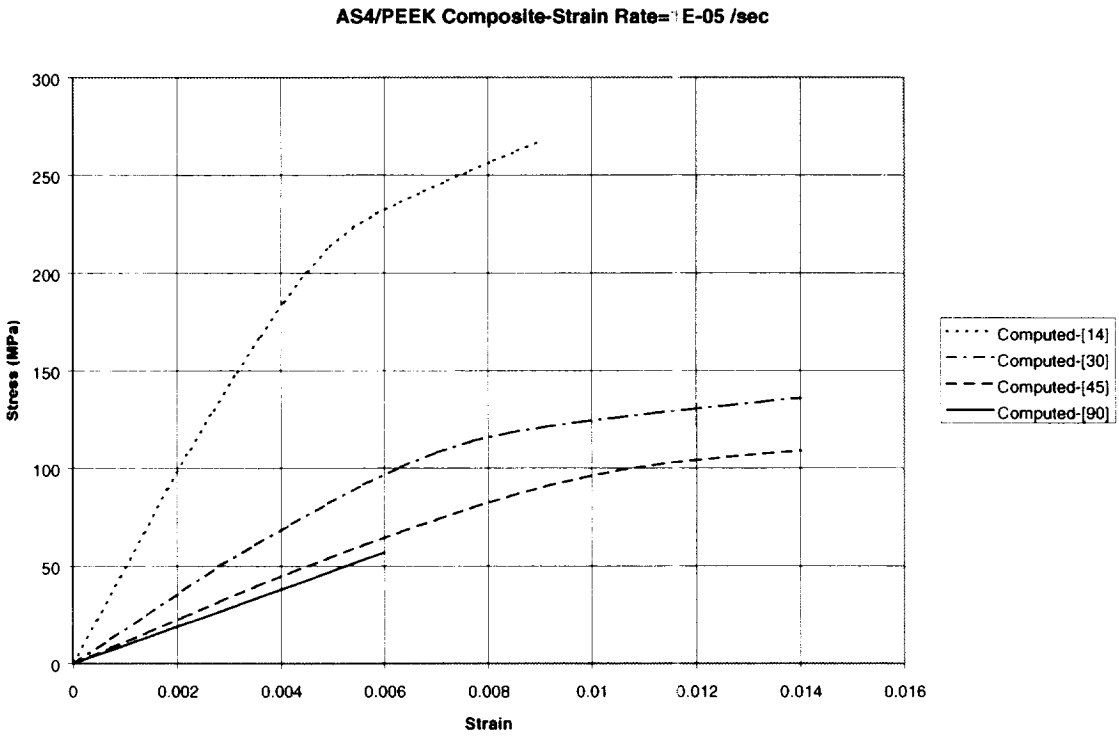

Figure 15: Model Predictions of Variation of Deformation Response of AS4/PEEK Composite with Fiber Orientation Angle-Strain Rate=1E-05 /sec

REPORT DOCUMENTATION PAGE

Form Approved
OMB No. 0704-0188

1. AGENCY USE ONLY (*Leave blank*)	2. REPORT DATE	3. REPORT TYPE AND DATES COVERED
	October 1998	Technical Memorandum

4. TITLE AND SUBTITLE

High Strain Rate Deformation Modeling of a Polymer Matrix Composite
Part II—Composite Micromechanical Model

5. FUNDING NUMBERS

WU-523-24-13-00

6. AUTHOR(S)

Robert K. Goldberg and Donald C. Stouffer

7. PERFORMING ORGANIZATION NAME(S) AND ADDRESS(ES)

National Aeronautics and Space Administration
Lewis Research Center
Cleveland, Ohio 44135-3191

8. PERFORMING ORGANIZATION REPORT NUMBER

E-11386

9. SPONSORING/MONITORING AGENCY NAME(S) AND ADDRESS(ES)

National Aeronautics and Space Administration
Washington, DC 20546-0001

10. SPONSORING/MONITORING AGENCY REPORT NUMBER

NASA TM—1998-208664

11. SUPPLEMENTARY NOTES

Robert K. Goldberg, NASA Lewis Research Center, and Donald C. Stouffer, University of Cincinnati, Cincinnati, Ohio 45221. Responsible person, Robert K. Goldberg, organization code 5920, (216) 433-3330.

12a. DISTRIBUTION/AVAILABILITY STATEMENT

Unclassified - Unlimited
Subject Category: 24 Distribution: Nonstandard

This publication is available from the NASA Center for AeroSpace Information, (301) 621-0390.

12b. DISTRIBUTION CODE

13. ABSTRACT ***(Maximum 200 words)***

Recently applications have exposed polymer matrix composite materials to very high strain rate loading conditions, requiring an ability to understand and predict the material behavior under these extreme conditions. In this second paper of a two part report, a three-dimensional composite micromechanical model is described which allows for the analysis of the rate dependent, nonlinear deformation response of a polymer matrix composite. Strain rate dependent inelastic constitutive equations utilized to model the deformation response of a polymer are implemented within the micromechanics method. The deformation response of two representative laminated carbon fiber reinforced composite materials with varying fiber orientation has been predicted using the described technique. The predicted results compare favorably to both experimental values and the response predicted by the Generalized Method of Cells, a well-established micromechanics analysis method.

14. SUBJECT TERMS

Composite materials; Impact; Micromechanics; Constitutive equations; Strain rate; Viscoplasticity

15. NUMBER OF PAGES

36

16. PRICE CODE

A03

17. SECURITY CLASSIFICATION OF REPORT	18. SECURITY CLASSIFICATION OF THIS PAGE	19. SECURITY CLASSIFICATION OF ABSTRACT	20. LIMITATION OF ABSTRACT
Unclassified	Unclassified	Unclassified	